Available online at www.sciencedirect.com

SciVerse ScienceDirect

journal homepage: www.elsevier.com/locate/he

Supported gold nanoparticles as anode catalyst for anion-exchange membrane-direct glycerol fuel cell (AEM-DGFC)

*Zhiyong Zhang, Le Xin, Wenzhen Li**

Department of Chemical Engineering, Michigan Technological University, 1400 Townsend Drive, Houghton, MI 49931, USA

ARTICLE INFO

Article history:
Received 25 January 2012
Received in revised form
22 February 2012
Accepted 5 March 2012
Available online 3 April 2012

Keywords:
Au
Nanoparticle
Electrooxidation
Glycerol
Alkaline electrolyte
Fuel cell

ABSTRACT

The carbon supported Au nanoparticles (Au-NPs) catalyst with a small average size (3.5 nm) and narrow size distribution (2–6 nm) was synthesized by a solution phase-based nanocapsule method. The reactivity of glycerol oxidation on Au/C is much higher than that of methanol and ethylene glycol oxidations in alkaline electrolyte. The anion-exchange membrane-direct glycerol fuel cell (AEM-DGFC) with the Au/C anode catalyst and a Fe-based cathode catalyst shows high performances with both high-purity glycerol and crude glycerol fuel: the open circuit voltages (OCVs) are 0.67 and 0.66 V, and peak power densities are 57.9 and 30.7 mW cm^{-2} at 80 °C, respectively. Fed with crude glycerol, the Au/C anode catalyst-based AEM-DGFC also demonstrates high performance stability at 80 °C. The product analysis shows that the electrooxidation of glycerol on the Au/C anode catalyst in AEM-DGFCs favors production of deeper-oxidized chemicals: tartronic acid, mesoxalic acid and oxalic acid, which leads to higher fuel cell's Faradic efficiency.

1. Introduction

The development of sustainable society needs wide-spread applications of renewable, reliable, and cost-effective energy technologies [1–3]. Fuel cells (FCs) are considered a promising alternative electric power device to meet humanity's energy demands [1,4]. Compared to H_2-fueled fuel cells, direct alcohol fuel cells (DAFCs) have attracted enormous attention due to the simple production, purification, and storage of the liquid fuels [5–8]. Among all the alcohols, the electrooxidation of methanol and ethanol have been widely investigated [9–14], due to their simple reaction mechanisms and relatively high theoretical energy density (4.8 and 6.4 kWh L^{-1}, respectively, for complete oxidation to CO_2). However, the toxicity of methanol and high volatility of ethanol, along with their low flash points remain critical issues under practical operation conditions [15]. Glycerol is a non-toxic, non-volatile, and non-flammable highly functionalized molecule with a theoretical energy density of 6.4 kWh L^{-1}. As a main byproduct of biodiesel production, glycerol is supplied in large quantities at low price (0.3 US$ kg^{-1}, crude glycerol) [16]. Therefore, glycerol is highly expected to be used in DAFCs as an inexpensive, renewable, and environmental-friendly fuel [17].

Various researches have been carried out in electrooxidation of glycerol in alkaline environment [7,18–22]. Matsuoka et al. first used glycerol as fuel in a PtRu/C anode catalyst-based anion-exchange membrane fuel cell (AEMFC),

* *Corresponding author*. Tel.: +1 906 487 2296; fax: +1 906 487 3213.
E-mail address: wzli@mtu.edu (W. Li).
0360-3199/$ – see front matter
doi:10.1016/j.ijhydene.2012.03.019

and obtained a peak power density of ~7 mW cm^{-2} at 50 °C [21]. Recently, Bianchini and co-workers achieved an AEM-DGFC performance of ~118 mW cm^{-2} on a Pd-(Ni–Zn–P)/C anode catalyst at 80 °C [7]. Very recently, based on a self-prepared Pt/C anode catalyst, our group also reported an AEM-DGFC performance of ~125 mW cm^{-2} at 80 °C [22]. However, most of the previous AEM-DGFC studies were focused on Pt- or Pd- based catalysts. Au has demonstrated high reactivity towards heterogeneous catalytic oxidation of glycerol [16,23–25]. However, due to the high onset potential (0.55–0.65 V *vs.* SHE) of glycerol electrooxidation observed on Au in three-electrode-cell studies [20,26], it was assumed that a very high overpotential would be inevitably observed on Au anode catalyst, and thus the fuel cell performance is largely lowered. Up to now, most previous research was focused on examining the mechanism and pathway of glycerol electro-oxidation [26,27]. No single cell performance has been reported on Au anode catalyst-based AEM-DGFCs.

Recently, we developed a novel solution phase-based nanocapsule method to precisely synthesize Pd/C and PdNi/C catalysts, which demonstrated high catalytic activity toward ethanol electrooxidation [28]. In this study, we modified this method to prepare carbon supported Au-NPs catalyst with a narrow particle size distribution of 2–6 nm. The Au/C catalyst was tested in a three-electrode cell setup, and further applied in an AEM-DGFC, demonstrating a high peak power density of 57.9 mW cm^{-2} at 80 °C. The AEM-DGFC with crude glycerol fuel under same test conditions also achieved an OCV of 0.66 V and a peak power density of 30.7 mW cm^{-2}. The product analysis reveals that in AEM-DGFC the Au/C anode catalyst favors the production of deeper-oxidized products, such as tartronic acid, mesoxalic acid, and oxalic acid. We further calculated the Faradic efficiency (η_e) of the AEM-DGFCs with the Au/C anode catalyst based on the product distributions.

2. Experimental section

2.1. Chemicals

$AuCl_3$ (Acros Organics), octadecene (Acros Organics), oleylamine (Aldrich), $LiBEt_3H$ (1 M in THF, Acros Organics), glycerol (99.8%, Fisher Scientific), methanol (99%, Sigma–Aldrich), EG (99%, BDH), and crude glycerol (88%, a byproduct from soy biodiesel manufacturing, Kingdom Bio Solutions Inc.) were used as purchased without further purification.

2.2. Preparation of Au/C catalyst

Au nanoparticles were synthesized through a modified solution-phase based nanocapsule method [28–34]. 0.5 mmol $AuCl_3$ (151.7 mg) was dissolved in a mixture of 16 ml octadecene and 4 ml oleylamine under a nitrogen flow. The system was then rapidly heated to 80 °C, subsequently followed by a quick injection of 1.5 ml $LiBEt_3H$. After holding the temperature for 10 min, the solution was cooled down to room temperature and separated by centrifugation. The as-prepared Au-NPs were deposited on 229.8 mg Vulcan XC-72R carbon black to make a 30 wt% Au/C catalyst.

2.3. Characterizations of Au/C catalyst

The morphology, structure, and metal loading of Au/C catalyst were analyzed by X-ray diffraction (XRD), transmission electron microscopy (TEM), and inductively coupled plasma atomic emission spectroscopy (ICP-AES). The XRD pattern was collected by a Scintag XDS-2000 θ/θ diffractometer with Cu K_α radiation (λ = 1.5406 Å), with a tube current of 35 mA and a tube voltage of 45 kV. TEM was performed by JEOL 2010 with an operating voltage of 200 kV. The Au particle size distribution was evaluated by 100 randomly chosen particles in an arbitrary area. 5.0 mg Au/C catalyst was dissolved in aqua regia (a strong acid mixture with HCl: HNO_3 volume ratio of 3:1) to form a Au aqueous solution, and ICP-AES was performed to detect the concentration of Au to obtain catalyst metal loading.

2.4. Half cell test

The half cell tests were performed in a conventional three-electrode-cell setup, with a glassy carbon working electrode, a Hg/HgO reference electrode and a Pt wire counter electrode. All potentials were given *vs.* Hg/HgO electrode (0.140 V vs. NHE) [35]. Before each test, 1.0 mg Au/C catalyst was dispersed in 1.0 ml isopropanol by sonication to form a uniform ink. The working electrode was prepared by dropping 20 μl of the ink on the glassy carbon electrode. 10 μl of 0.05 wt% AS-4 (Tokuyama) ionomer solution was added on the top to fix the catalyst. The electrochemical surface area (ECSA) of the Au/C catalyst was studied by a cyclic voltammetry (CV) test from −0.9–0.7 V in 1.0 M KOH with a scan rate of 50 m Vs^{-1}, and was calculated based on the reduction peak of a monolayer of gold oxide. The activity of glycerol electrooxidation was investigated in 2.0 M KOH + 0.05 M glycerol by a 10-cycle-CV scan from −0.9–0.8 V at the same scan rate. The result was compared with that of methanol and EG under the same test condition. In order to further optimize the effects of alkaline and glycerol concentrations, linear scan voltammetry (LSV) was carried out in different concentrations of KOH and glycerol from −0.9–0.8 V, with a scan rate of 1 m Vs^{-1} and a rotation speed of 2500 rpm.

2.5. MEA fabrication and AEM-DGFC test

A catalyst ink containing 90 wt% of as-prepared Au/C catalyst (30 wt%) and 10 wt% of Teflon was sprayed on a carbon cloth anode liquid diffusion layer, to obtain an anode with catalyst loading of 1.0 mg_{Au} cm^{-2}. On the cathode, a commercial non-Pt group metal (PGM) HYPERMECTM catalyst (Fe–Cu–N_4/C, Acta) was blended with AS-4 anion conductive ionomer (Tokuyama), and sprayed directly onto the A201 membrane to obtain a catalyst loading of 1.0 $mg_{cat.}cm^{-2}$. The membrane was then covered with a 25 CC carbon paper (SGL Group) cathode gas diffusion layer and assembled with the Au/C-based anode into an MEA with an active cross-sectional area of 5 cm^2. The performance of AEM-DGFC was evaluated with a 2.0 M KOH + 1.0 M glycerol solution and high-purity O_2 (99.999%) at a constant flow rate of 0.4 L min^{-1} under 30 psi back pressure, from 50 to 80 °C. Served as control experiments, the performances of AEMFCs fed with 2.0 M KOH + 1.0 M methanol (or EG) were also investigated at 80 °C. In order to examine the

performance of biomass-derived crude glycerol in Au/C anode catalyst-based AEM-DGFC, 2.0 M KOH + 1.0 M crude glycerol was applied as fuel at 80 °C. The performance stability of Au/C anode catalyst-based AEM-DGFC fed with crude glycerol was studied by 100 continuous runs of polarization scans under the same test conditions, while the cathode catalyst loading was increased to 2.0 mg cm^{-2} to minimize the effect of cathode catalyst activity loss.

2.6. *Product analysis*

Qualitative analyses of the products at different cell operation voltages were carried out using an HPLC (Agilent 1100) with a refractive index detector (RID, G1326A, Agilent). The samples were separated using an OA-1000 column (Alltech) at 60 °C with an eluent of 5 mM aqueous sulfuric acid (0.3 ml min^{-1}). Products were identified by comparison with authentic samples.

3. Results and discussion

The XRD pattern of Au/C catalyst is shown in Fig. 1, which presents a typical Au face centered cubic (FCC) structure (JCPDS card 4-784). The average Au crystal size calculated based on the Au (220) diffraction peak is 3.4 nm, using the Debye-Scherer formula as shown below [36]:

$$L = \frac{0.9\lambda_{K\alpha}}{B_{2\theta}\cos\theta_{max}} \quad (1)$$

where L is the mean crystal size, λ is the wavelength of the x-ray (1.5406 Å), B is the full width at half-maximum of the peak (rad) and θ_{max} is the Bragg angle (rad) of Pt (220).

A typical TEM image of Au/C is shown in Fig. 2a. It is evidenced that most Au-NPs are round and uniformly dispersed on the carbon support with only a few agglomerations. The Au average particle size measured from the TEM image is 3.5 nm, showing a good agreement with the XRD result. The histogram of particle sizes evaluated from over 100 particles in an arbitrarily chosen area is shown in Fig. 2b and suggests

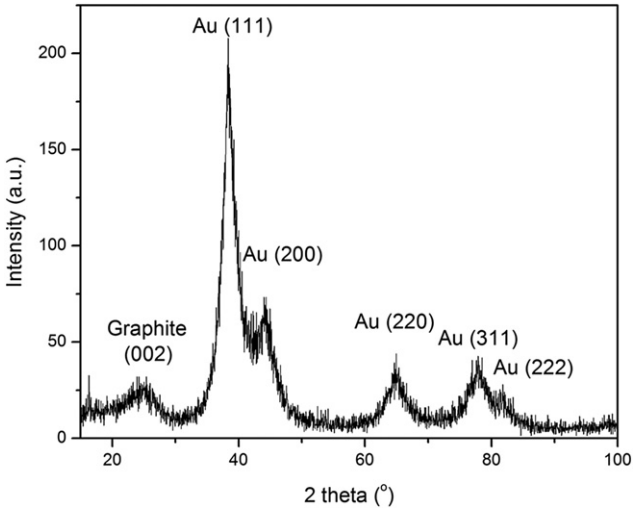

Fig. 1 – XRD pattern of Au/C catalyst.

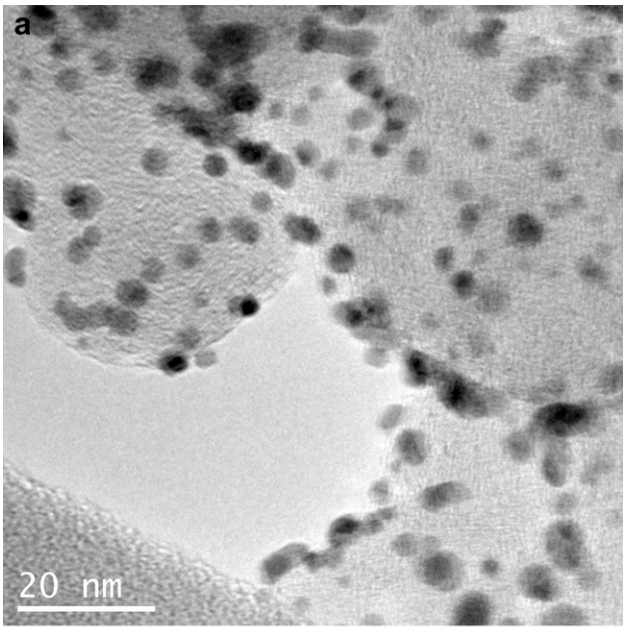

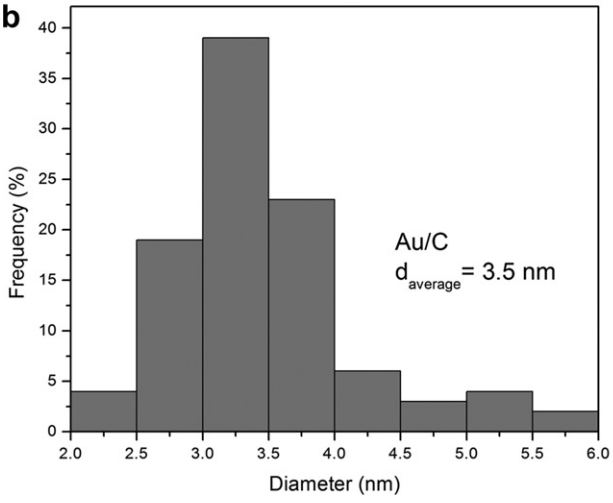

Fig. 2 – TEM image (a), and particle size histogram (b) of Au/C.

a narrow size distribution of 2–6 nm. The metal loading determined by ICP-AES is 30.8 wt%, indicating all the Au precursor was fully reduced and deposited on the carbon support. Compared to previous studies [37–39], our self-prepared Au/C catalyst exhibits a smaller diameter and a narrow size distribution, indicating that the nanocapsule method has a better morphology control capability on Au, even with a high metal loading of 30 wt%.

In order to obtain the ECSA of the as-prepared Au/C catalyst, a 10-cycle CV scan was performed in 1.0 M KOH from −0.9–0.7 V at 50 mV s^{-1}, and the last cycle is shown in Fig. 3a. The anodic peak on the forward scan and the cathodic peak on the backward scan are assigned to the formation and reduction of a monolayer of Au oxide [40]. The ECSA of Au/C catalyst is 26.8 m^2 g^{-1}, which was evaluated from the reduction peak at ~0.13 V with a double layer correction and a charge density of 0.386 mC cm^{-2} [40].

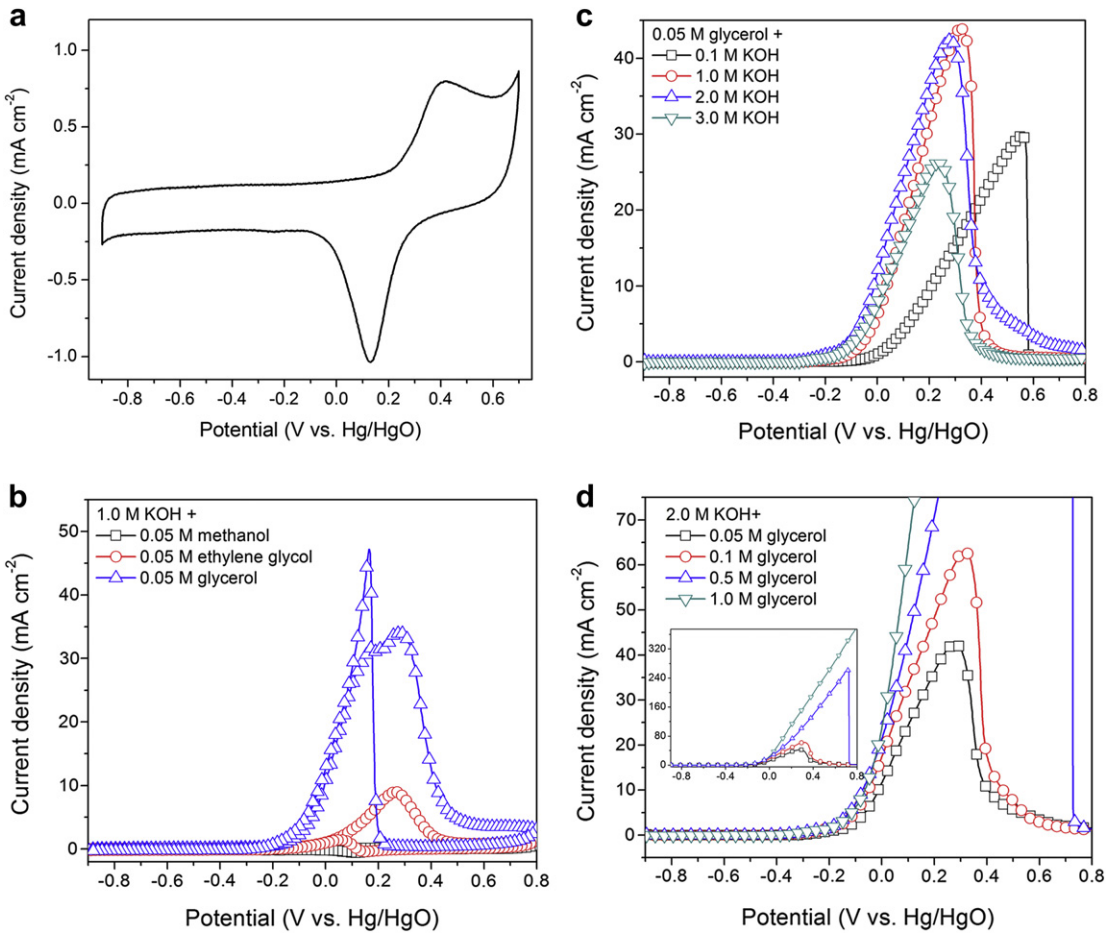

Fig. 3 – Cyclic voltammograms of Au/C in 1.0 M KOH, 50 mV s^{-1} (a), 1.0 M KOH + 0.05 M alcohols, 50 mV s^{-1} (b), 0.05 M glycerol + 0.1–3.0 M KOH, 1 mV s^{-1} (c), and 2.0 M KOH + 0.05 M–1.0 M glycerol, 1 mV s^{-1}, the inserted zooming out current in y-axis (d), at room temperature.

The electrocatalytic oxidation of glycerol in alkaline media on Au/C was investigated in 1.0 M KOH + 0.05 M glycerol, and was compared with that of methanol and ethylene glycol (EG) under the same condition. As shown in Fig. 3b, the shape of CV curves of both EG and glycerol oxidation represents the typical electrooxidation reaction of alcohols, with two well-defined anodic peaks in forward and backward scans. However, the electrooxidation of methanol is weak on Au/C. It is interesting that the glycerol oxidation current is less stable than EG oxidation current in range of 0.16–0.3 V, which may be attributed to the complex electrooxidation kinetics [20]. Compared to EG and methanol, glycerol possesses a higher activity on Au/C catalyst, with both a lower onset potential and higher electrooxidation currents in the whole investigated potential range. Based on the base catalysis theory, the first deprotonation of H_α in alcohol on Au catalyst is base catalyzed [41]:

$$H_\beta R - OH_\alpha + OH^- \rightleftarrows H_\beta R - O^- + H_2O \quad (2)$$

The reaction produces highly reactive alkoxide and follows a Hammett type correlation with the pK_a of alcohol. Therefore, a lower pK_a of alcohol will lead to a higher reactivity. As the pK_a of glycerol is 14.15, which is lower than that of EG (14.77) and methanol (15.50), it is easier for glycerol to deprotonate into highly reactive glycerolate in high pH media, resulting in a high overall electrooxidation activity. Therefore, glycerol is expected to be a promising fuel for Au anode catalyst-based AEM-DGFC.

The effect of alkaline concentration on glycerol electrooxidation was further investigated through linear voltammetry scans with 0.05 M glycerol, and the results are shown in Fig. 3c. It is reasonable to consider that the glycerol oxidation on the Au/C undergoes a quasi-steady state with negligible mass transfer issue, due to the adopted slow scan rate of 1 mV s^{-1} and high electrode rotation speed of 2500 rpm. With the KOH concentration increasing, the onset potential of glycerol oxidation shifts negatively, with the value of −0.271, −0.274, and −0.374 V in 0.1, 1.0, and 2.0 M KOH, respectively. It was reported that high pH will benefit the initial deprotonation of glycerol [42,43]. Therefore, high OH^- concentration will promote the generation of highly reactive glycerolate through a simple base catalyzed pathway in the electrolyte [41]. Meanwhile, recent investigation of DFT calculation also suggests that in an alkaline environment, the adsorbed OH_{ad} will enhance the elimination of both H_α and H_β of adsorbed alcohols on the Au surface through a metal surface catalyzed

process by lowing the activation energy barriers [23], as shown in Eqs (3) and (4), respectively:

$$H_\beta R - OH_{\alpha,ad} + OH_{ad} \rightarrow H_\beta R - O_{ad} + H_2O \quad (3)$$

$$H_\beta R - O_{ad} + OH_{ad} \rightarrow R = O_{ad} + H_2O \quad (4)$$

The higher pH will increase the OH_{ad} coverage rate on the Au surface and facilitate glycerol electrooxidation. Also, according to the bi-functional theory, oxidation of primary alcohol requires adsorbed OH on the catalyst surface to decrease the onset potential [20], which will take advantage of high pH electrolytes [44]. It is worthy to point out when the concentration of KOH further increases to 3.0 M, the onset potential shifts positively to −0.354 V. This is probably because too much OH_{ad} on the Au catalyst surface blocks the glycerol adsorption, resulting in a lower reactivity. The OH^- concentration also affects the peak current and peak potential. In the case of KOH > 1.0 M, it has been found that the high OH_{ad} coverage ratio leads to an insufficient glycerol and/or alkoxy adsorption, which further results in a lower current density. In the meantime, it is noted that the peak potential shifts to the negative direction with OH^- concentration increasing. Although this peak shift was assigned by some authors to be an enhancement of glycerol oxidation reactivity [20], previous studies of surface Au oxidation in alkaline electrolyte revealed that the sharp decrease in the oxidation currents was due to the formation of a well-developed gold oxide layer [27,45]. Therefore, the peak shifts may indicate that high OH_{ad} coverage will enhance the generation of a fully developed Au oxide layer at the catalyst surface.

Fig. 3d shows the electrooxidation curves of different concentration of glycerol in 2.0 M KOH. With the glycerol concentration increasing, the onset potential gradually shifts to the negative direction, with the value of −0.374, −0410, −0.460 and −0.480 V for 0.05, 0.1, 0.5 and 1.0 M glycerol, respectively. As glycerol is a weak acid with a pKa = 14.15, higher glycerol concentration will generate more highly reactive glycerolate, that will further improve the onset potential. With the glycerol concentration increasing, the peak position moves monotonically to the positive direction, leading to higher peak currents. Higher initial glycerol concentration can lead to higher alkoxy or other intermediates adsorbed on the Au surface, which will reduce the OH_{ad} coverage ratio, therefore, delay the formation of gold oxide layer on the catalyst surface. On the other hand, some intermediates, ie, alkoxy and aldehyde, with high reducing activity, could 'protect' the surface Au from being oxidized and losing reactivity. 1.0 M glycerol is such a high concentration that no peak current could be found in the whole investigated potential range.

The as-prepared Au/C was applied as the anode catalyst for an AEM-DGFC, and demonstrated high electricity generation performance. As shown in Fig. 4a, when fed with 2.0 M KOH + 1.0 M glycerol, the AEM-DGFC with a loading of 1.0 mg_{Au} cm^{-2} produced an open circuit voltage (OCV) of 0.59 V and a peak power density of 17.5 mW cm^{-2} at 110 mA cm^{-2} at 50 °C. The performance was significantly improved with the temperature increasing. At higher temperatures of 60 and 70 °C, the OCV and peak power density reached 0.63 V and 26.3 mW cm^{-2} (at 130 mA cm^{-2}), and 0.65 V and 37.1 mW cm^{-2}(at 190 mA cm^{-2}), respectively. When the temperature further increasing to 80 °C, the OCV achieved at 0.67 V, while the peak power density reached 57.9 mW cm^{-2}. In addition, as the operation temperature was increased, the slope of I–V curve became less negative at the electrochemical kinetics-controlled low current density region (i.e. 0–50 mA cm^{-2}), indicating the glycerol oxidation kinetics were greatly enhanced at higher temperatures. It is also demonstrated in Fig. 4a that the mass transport limiting currents increased from 210 mA cm^{-2} (50 °C) to 389 mA cm^{-2} (80 °C), indicating that better reactant diffusion may be achieved at higher temperatures. The output power density observed in the Au/C anode catalyst-based AEM-DGFC is 1–2 orders higher than the state-of-art biofuel cells with glycerol fuel (normally < 1.0 mW cm^{-2}) [46,47]. It is also much higher than the performance of PtRu/C anode catalyst-based (2.6 mW cm^{-2} on 4.0 mg_{PtRu} cm^{-2}) proton-exchange membrane-direct glycerol fuel cell (PEM-DGFC). The promising performance of this AEM-DGFC may be attributed to the small Au nanoparticles (2–6 nm), which offers a high active surface area, and increased number of Au atoms with higher intrinsic activity at the edge [42,48,49].

The behavior of AEM-DGFC is also compared with that of AEMFCs fed with methanol and EG under the same test conditions at 80 °C, as shown in Fig. 4b. When fed with 2.0 M KOH + 1.0 M methanol, the AEMFC only yielded an OCV of 0.29 V and an peak power density of 0.8 mW cm^{-2}(at 8 mA cm^{-2}). With the number of hydroxymethyl groups in the fuel molecules increasing, the OCV and peak power density increased significantly: 0.58 V and 20.3 mW cm^{-2} for 1.0 M EG, and 0.67 V and 57.9 mW cm^{-2} for 1.0 M glycerol. At the same time, the better oxidation kinetics of alcohols with more hydroxymethyl groups are also evidenced by the increase of limiting current, as well as the less steep slope of I–V curve at low current density region. The AEMFC performances with different alcohols are in good agreement with the half cell test results, with the reactivity sequence of glycerol > EG > methanol.

A commercial crude glycerol was directly employed as fuel for the Au/C anode catalyst-based AEM-DGFC, which demonstrated reasonably high performance at 80 °C. The crude glycerol contains 88.05 wt.% of glycerol, 5.42 wt.% of matter organic non glycerol (MONG), 4.16 wt.% of moisture, 2.37 wt.% of ash, and 628 ppm of methanol, and was used as purchased without any further treatment. As shown in Fig. 4c, when fed with 2.0 M KOH + 1.0 M crude glycerol, the OCV and peak power density of the AEM-DGFC reached 0.66 V and 30.7 mW cm^{-2} (at 140 mA cm^{-2}) at 80 °C. The fuel cell performance with crude glycerol is comparable to that with high-purity glycerol (0.67 V and 57.9 mW cm^{-2}) and higher than that with high-purity EG (0.58 V and 20.3 mW cm^{-2}). This indicates that Au/C is able to serve as a highly active anode catalyst for electrooxidation of biomass-derived crude glycerol in AEM-DGFC, without being significantly poisoned by the impurities.

The Au/C anode catalyst-based AEM-DGFC with crude glycerol also demonstrates high performance stability. Fed with 2.0 M KOH + 1.0 M crude glycerol, the durability of Au/C anode AEM-DGFC was tested through 100 continuous runs of polarization scans at 80 °C. The cathode loading was increased to 2.0 mg cm^{-2} to minimize the effect of cathode catalyst activity loss within the long-term test at the elevated

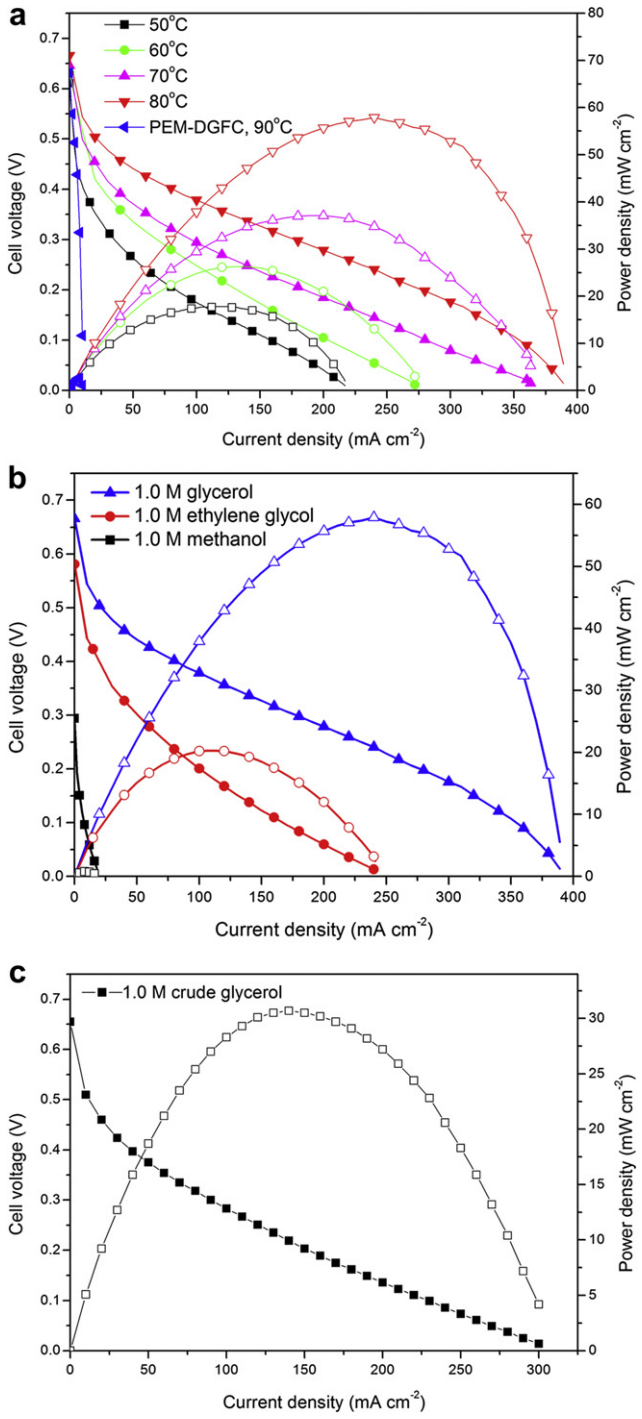

Fig. 4 – Polarization curves of an AEM-DGFC at operation temperature of 50, 60, 70, and 80 °C, and a proton-exchange membrane direct glycerol fuel cell (PEM-DGFC) at 90 °C (a), AEMFCs fed with methanol, EG and glycerol at 80 °C (b), and AEM-DGFC fed with crude glycerol at 80 °C (c). Test conditions for AEM-DGFC: Anode: Au/C (1.0 mg_{Au} cm^{-2}), 2.0 M KOH + 1.0 M alcohol, 4.0 mL min^{-1}, cathode: Fe–Cu–N_4/C (Acta 4020, 1.0 mg cm^{-2}), O_2, 0.4 L min^{-1}, 30 psi, AEM: A201 (28 μm, Tokuyama). Test conditions for PEM-DGFC: Anode: PtRu/C (4.0mg_{PtRu} cm^{-2}), 1.0 M glycerol, 4.0 mL min^{-1}, cathode: Pt/C (4.0mg_{Pt} cm^{-2}), O_2, 0.4 L min^{-1}, 30 psi, PEM: Nafion 115 (150 μm, Dupont).

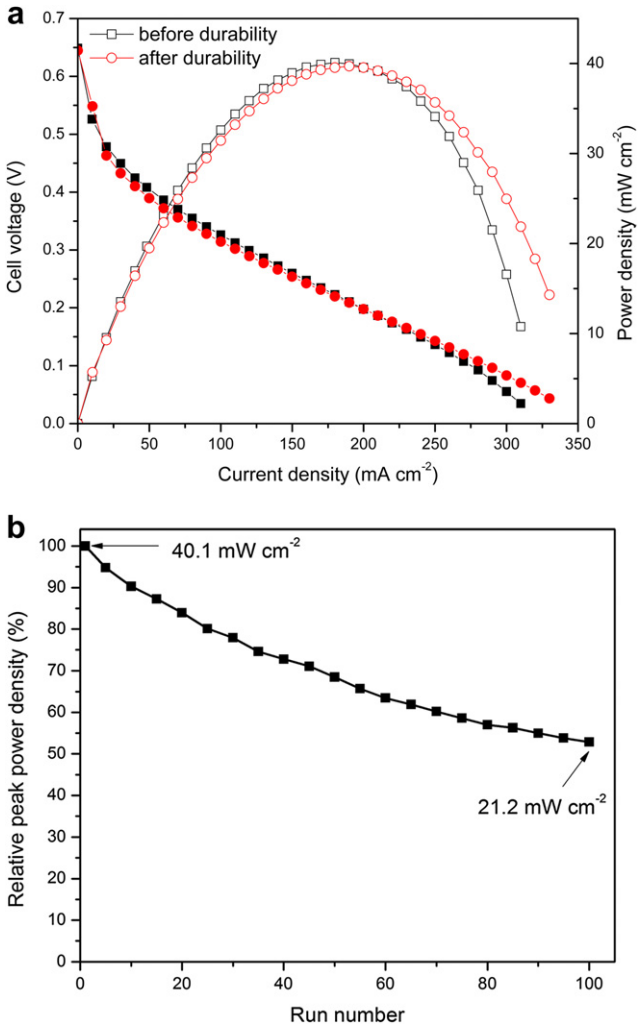

Fig. 5 – Polarization curves of an AEM-DGFC before and after the durability test (a), and the relative peak power density losses within the durability test (b), fed with 2.0 M KOH + 1.0 M crude glycerol. Test conditions: Anode: Au/C (1.0 mg_{Au} cm^{-2}), 4.0 mL min^{-1}, cathode: Fe–Cu–N_4/C (Acta 4020, 2.0 mg cm^{-2}), O_2, 0.4 L min^{-1}, 30 psi, AEM: A201 (28 μm, Tokuyama), 80 °C.

temperature of 80 °C. The initial polarization curve (before the durability test) in Fig. 5a shows a peak power density of 40.1 mW cm^{-2}, which is ~10 mW cm^{-2} higher than the performance in Fig. 4c due to the increase of cathode catalyst loading. The relative peak power densities during the durability test are plotted in Fig. 5b, which gradually dropped to 53% of its original value (21.2 mW cm^{-2}) after 100 continuous runs. The decrease of peak power density is probably due to the reaction intermediates/poisons generated during the long-term reaction blocked Au surface active sites. After the durability test, the anode was cleaned by flushing with de-ionized water, and the fuel cell performance was tested again under the same conditions. As shown in Fig. 5a, the polarization curve demonstrates no drop in electricity generation performance even after 100 continuous runs of durability test, indicating a high stability of the Au/C anode

Table 1 – Product selectivity and faradic efficiency (η_e) of an AEM-DGFC with Au/C anode catalyst under different fuel cell working voltages.

Cell voltage (V)	Selectivity (%)					η_e (%)
	Glyceric acid	Tartronic acid	Mesoxalic acid	Glycolic acid	Oxalic acid	
0.5	26	49	0	0	25	53.3
0.3	17	39	19	0	25	58.6
0.1	26	37	12	3	22	54.1

catalyst. It is noted that after the durability test, the limiting current increased from 310 mA cm^{-2} to 330 mA cm^{-2}, which implies better reactant diffusion was achieved.

To investigate the glycerol electrooxidation products on Au/C anode catalyst in AEM-DGFC and the fuel cell's Faradic efficiency, 55 ml 2.0 M KOH + 1.0 M glycerol was continuously looped from a plastic vessel into the anode, while a constant cell voltage (0.5, 0.3, or 0.1 V) was applied for 2 h at 50 °C. Table 1 presents the products selectivities analyzed by HPLC under different fuel cell operation voltages. The selectivity (S) is defined as the moles of product divided by the moles of C_2 and C_3 products observed at the given time (2 h) [23,43]. Although the previous studies of glycerol electrooxidation in traditional three-electrode system by other groups indicate that Au only produces lightly oxidized products, such as glyceric acid and glycolic acid [26,50], our investigation found that the Au/C anode catalyst in AEM-DGFC more favors the generation of deeper-oxidized products, tartronic acid (37%–49%) and oxalic acid (22%–25%) in the whole fuel cell operation voltage range. At lower cell voltages, the fully oxidized C_3 acid- mesoxalic acid was also detected with the selectivity of 19% and 12%, at 0.3 and 0.1 V, respectively. This is in sharp contrast to heterogeneous catalytic partial oxidation of glycerol over Au/C catalysts, through which the main product is glyceric acid. i.e. Hutchings' group reported a 100% glyceric acid selectivity under an optimized condition [24]. The high selectivity of deeper-oxidized products on Au/C in the AEM-DGFC may be attributed to the high catalyst loading and the unique carbon cloth-based liquid diffusion layer, which will elongate the fuel residence time inside the catalyst layer and allow glycerol to undergo deeper oxidations.

Based on the product distributions, the Faradic efficiency (η_e), which is defined as the ratio of transferred electrons in the partial oxidation to that in the complete oxidation (combustion to CO_2), was calculated by the following equation:

$$\eta_e = \sum S_i \cdot \eta_{e_i} \quad (5)$$

where S_i is the selectivity of product i, and η_{ei} is the Faradic efficiency of partial oxidation product. The higher Faradic efficiency means more electrons are exploited from the fuel, and thus represents a greater utilized fuel energy density. Since full oxidization of glycerol to CO_2 yields 14 electrons, the Faradic efficiencies of partial oxidizing glycerol to glyceric acid (4e), tartronic acid (8e), mesoxalic acid (10e), glycolic acid (6e), and oxalic acid (10 e) are 28.6%, 57.1%, 71.4%, 42.9%, and 71.4%, respectively. The calculation is based on that all the C_1 product is formic acid, which is a reasonable assumption supported by a recent study, which shows Au is nearly inert to further oxidize formic acid to carbonate [50]. As shown in Table 1, the Faradic efficiencies at fuel cell operation voltages of 0.5, 0.3, and 0.1 V are calculated to be 53.3%, 58.6%, and 54.1%, respectively, as shown in Table 1. By comparison, the main oxidation product for direct ethanol fuel cells (DEFCs, ethanol is another important biorenewable alcohol) is acetic acid or acetaldehyde even on the Pt/C or PtSn/C anode catalyst, due to the difficulty of C–C bond cleavage [5,7]. Therefore, the Faradic efficiency of a DEFC drops down to only 33.3% (acetic acid), and 16.7% (acetaldehyde). The AEM-DGFC with Au/C anode catalyst has a great advantage in exploiting more electrons from glycerol during its electrooxidation, and thus improves the fuel efficiency. In order to further improve the catalytic reactivity and reduce the large anode overpotential, development of Au-based bimetallic catalysts with higher catalytic reactivity is currently underway in our lab.

4. Conclusions

In this study, carbon supported Au-NPs catalyst with a small average size of 3.5 nm was successfully prepared by a modified nanocapsule method. The reactivity of glycerol oxidation on Au/C is much higher than that of methanol and EG oxidation in alkaline electrolyte. A subtle balance of glycerol and OH^- concentration is required to obtain a high electrooxidation reactivity. The Au/C catalyst has demonstrated a high performance in AEM-DGFC: at 80 °C, the OCV and peak power density can reach 0.67 V and 57.9 mW cm^{-2}, respectively. Even directly fed with crude glycerol, the OCV and peak power density of the AEM-DGFC can still achieve 0.66 V and 30.7 mW cm^{-2}, respectively. The Au/C anode catalyst-based AEM-DGFC also demonstrates high performance stability: after 100 runs of polarization scans at 80 °C, it shows no obvious performance loss when fed with 2.0 M KOH + 1.0 M crude glycerol. The product analysis shows electrooxidation of glycerol on the Au/C anode catalyst in AEM-DGFCs favors the formation of deeper-oxidized products: tartronic acid, mesoxalic acid and oxalic acid, which leads to higher fuel cell's Faradic efficiency.

Acknowledgement

We acknowledge the US National Science Foundation (CBET-1032547) for funding. Acknowledgment is also made to the Donors of the American Chemical Society Petroleum Research Fund for partial support of this research. W. Li thanks the support from Michigan Tech Research Excellence Fund - Research Seeds (REF-RS) grant E49236. We are grateful to Profs. Susan Bagley and David Shonnard for their help with our HPLC analysis.

REFERENCES

[1] Dresselhaus MS, Thomas IL. Alternative energy technologies. Nature 2001;414:332–7.
[2] Huber GW, Iborra S, Corma A. Synthesis of transportation fuels from biomass: chemistry, catalysts, and engineering. Chemical Reviews 2006;106:4044–98.
[3] Kamat PV. Meeting the clean energy demand: nanostructure architectures for solar energy conversion. Journal of Physical Chemistry C 2007;111:2834–60.
[4] Steele BC, Heinzel A. Materials for fuel-cell tenologies. Nature 2001;414:345–52.
[5] Lamy C, Coutanceau C, Leger J-M. The direct ethanol fuel cell: a challenge to convert bioethanol Cleanly into electric energy. In: Catalysis for sustainable energy production. Wiley-VCH Verlag GmbH & Co. KGaA; 2009. 1–46.
[6] Aricò AS, Baglio V, Antonucci V. Direct methanol fuel cells: History, Status and Perspectives. In: Electrocatalysis of direct methanol fuel cells. Wiley-VCH Verlag GmbH & Co. KGaA; 2009. 1–78.
[7] Bianchini C, Shen PK. Palladium-Based electrocatalysts for alcohol oxidation in half cells and in direct alcohol fuel cells. Chemical Reviews 2009;109:4183–206.
[8] Antolini E, Gonzalez ER. Alkaline direct alcohol fuel cells. Journal of Power Sources 2010;195:3431–50.
[9] Zhou WJ, Zhou ZH, Song SQ, Li WZ, Sun GQ, Tsiakaras P, et al. Pt based anode catalysts for direct ethanol fuel cells. Applied Catalysis B-Environmental 2003;46: 273–85.
[10] Wang Q, Sun GQ, Jiang LH, Xin Q, Sun SG, Jiang YX, et al. Adsorption and oxidation of ethanol on colloid-based Pt/C, PtRu/C and Pt3Sn/C catalysts: in situ FTIR spectroscopy and on-line DEMS studies. Physical Chemistry Chemical Physics 2007;9:2686–96.
[11] Han S, Song Y, Lee J, Kim J, Park K. Platinum nanocube catalysts for methanol and ethanol electrooxidation. Electrochemistry Communications 2008;10:1044–7.
[12] Fengping H, Guofeng C, Zidong W, Pei Kang S. Improved kinetics of ethanol oxidation on Pd catalysts supported on tungsten carbides/carbon nanotubes. Electrochemistry Communications; 2008:1303–6.
[13] Liu HP, Ye JP, Xu CW, Jiang SP, Tong YX. Kinetics of ethanol electrooxidation at Pd electrodeposited on Ti. Electrochemistry Communications 2007;9:2334–9.
[14] Shen PK, Xu CW. Alcohol oxidation on nanocrystalline oxide Pd/C promoted electrocatalysts. Electrochemistry Communications 2006;8:184–8.
[15] Matsuoka K, Iriyama Y, Abe T, Matsuoka M, Ogumi Z. Electro-oxidation of methanol and ethylene glycol on platinum in alkaline solution: Poisoning effects and product analysis. Electrochimica Acta 2005;51:1085–90.
[16] Katryniok B, Kimura H, Skrzynska E, Girardon J-S, Fongarland P, Capron M, et al. Selective catalytic oxidation of glycerol: perspectives for high value chemicals. Green Chemistry 2011;13:1960–79.
[17] Kim HJ, Choi SM, Green S, Tompsett GA, Lee SH, Huber GW, et al. Highly active and stable PtRuSn/C catalyst for electrooxidations of ethylene glycol and glycerol. Applied Catalysis B-Environmental 2011;101:366–75.
[18] Yu EH, Krewer U, Scott K. Principles and Materials Aspects of direct alkaline alcohol fuel cells. Energies 2010;3: 1499–528.
[19] Roquet L, Belgsir EM, Leger JM, Lamy C. Kinetics and mechanisms of the electrocatalytic oxidation of glycerol as investigated by Chromatographic analysis of the reaction-products - Potential and Ph effects. Electrochimica Acta 1994; 39:2387–94.
[20] Simoes M, Baranton S, Coutanceau C. Electro-oxidation of glycerol at Pd based nano-catalysts for an application in alkaline fuel cells for chemicals and energy cogeneration. Applied Catalysis B-Environmental 2010;93:354–62.
[21] Matsuoka K, Iriyama Y, Abe T, Matsuoka M, Ogumi Z. Alkaline direct alcohol fuel cells using an anion exchange membrane. Journal of Power Sources 2005;150:27–31.
[22] Zhang Z, Xin L, Li W. Electrocatalytic oxidation of glycerol on Pt/C in anion-exchange membrane fuel cell: cogeneration of electricity and valuable chemicals. Applied Catalysis B Environmental 2012;119-120:40–8.
[23] Zope BN, Hibbitts DD, Neurock M, Davis RJ. Reactivity of the Gold/Water Interface during Selective oxidation catalysis. Science 2010;330:74–8.
[24] Carrettin S, McMorn P, Johnston P, Griffin K, Hutchings GJ. Selective oxidation of glycerol to glyceric acid using a gold catalyst in aqueous sodium hydroxide. Chemical Communications 2002:696–7.
[25] Pagliaro M, Ciriminna R, Kimura H, Rossi M, Della Pina C. From glycerol to value-added products. Angewandte Chemie-International Edition 2007;46:4434–40.
[26] Kwon Y, Koper MTM. Combining voltammetry with HPLC: application to Electro-oxidation of glycerol. Analytical Chemistry 2010;82:5420–4.
[27] Jeffery DZ, Camara GA. The formation of carbon dioxide during glycerol electrooxidation in alkaline media: first spectroscopic evidences. Electrochemistry Communications 2010;12:1129–32.
[28] Zhang Z, Xin L, Sun K, Li W. Pd–Ni electrocatalysts for efficient ethanol oxidation reaction in alkaline electrolyte. International Journal of Hydrogen Energy 2011;36: 12686–97.
[29] Li WZ, Haldar P. Supportless PdFe nanorods as highly active electrocatalyst for proton exchange membrane fuel cell. Electrochemistry Communications 2009;11:1195–8.
[30] Li WZ, Chen ZW, Xu LB, Yan Y. A solution-phase synthesis method to highly active Pt-Co/C electrocatalysts for proton exchange membrane fuel cell. Journal of Power Sources 2010; 195:2534–40.
[31] Li WZ, Haldar P. Highly active carbon supported Core-Shell PtNi@Pt nanoparticles for oxygen reduction reaction. Electrochemical and Solid State Letters 2010;13:B47–9.
[32] Li WZ, Xin Q, Yan YS. Nanostructured Pt-Fe/C cathode catalysts for direct methanol fuel cell: the effect of catalyst composition. International Journal of Hydrogen Energy 2010; 35:2530–8.
[33] Zhang Z, More KL, Sun K, Wu Z, Li W. Preparation and Characterization of PdFe Nanoleaves as electrocatalysts for oxygen reduction reaction. Chemistry of Materials 2011;23: 1570–7.
[34] Zhang ZY, Li MJ, Wu ZL, Li WZ. Ultra-thin PtFe-nanowires as durable electrocatalysts for fuel cells. Nanotechnology 2011;22.
[35] Potentials of Common Reference Electrodes. http://www.consultrsr.com/resources/ref/refpotls.htm.
[36] Winjobi O, Zhang ZY, Liang CH, Li WZ. Carbon nanotube supported platinum-palladium nanoparticles for formic acid oxidation. Electrochimica Acta 2010;55:4217–21.
[37] Bianchi CL, Canton P, Dimitratos N, Porta F, Prati L. Selective oxidation of glycerol with oxygen using mono and bimetallic catalysts based on Au, Pd and Pt metals. Catalysis Today 2005;102:203–12.
[38] Zhang S, Shao Y, Yin G, Lin Y. Electrostatic self-Assembly of a Pt-around-Au Nanocomposite with high activity towards formic acid oxidation. Angewandte Chemie International Edition 2010;49:2211–4.
[39] Yan S, Zhang S. Investigation of methanol electrooxidation on Au/C catalyst in alkaline medium. International Journal of Hydrogen Energy 2011;36:13392–7.

[40] Burke LD, Moran J, Nugent P. Cyclic voltammetry responses of metastable gold electrodes in aqueous media. Journal of Solid State Electrochemistry 2003;7:529–38.
[41] Koper MTM, Kwon Y, Lai SCS, Rodriguez P. Electrocatalytic oxidation of alcohols on gold in alkaline media: base or gold catalysis? Journal of the American Chemical Society 2011; 133:6914–7.
[42] Carrettin S, McMorn P, Johnston P, Griffin K, Kiely CJ, Attard GA, et al. Oxidation of glycerol using supported gold catalysts. Topics in Catalysis 2004;27:131–6.
[43] Ketchie WC, Murayama M, Davis RJ. Promotional effect of hydroxyl on the aqueous phase oxidation of carbon monoxide and glycerol over supported Au catalysts. Topics in Catalysis 2007;44:307–17.
[44] Chen AC, Lipkowski J. Electrochemical and spectroscopic studies of hydroxide adsorption at the Au(111) electrode. Journal of Physical Chemistry B 1999;103:682–91.
[45] de Lima RB, Varela H. Catalytic oxidation of ethanol on gold electrode in alkaline media. Gold Bull 2008;41:15–22.
[46] Arechederra RL, Treu BL, Minteer SD. Development of glycerol/O-2 biofuel cell. Journal of Power Sources 2007;173: 156–61.
[47] Arechederra RL, Minteer SD. Complete oxidation of glycerol in an Enzymatic biofuel cell. Fuel Cells 2009;9:63–9.
[48] Ketchie W, Fang Y, Wong M, Murayama M, Davis R. Influence of gold particle size on the aqueous-phase oxidation of carbon monoxide and glycerol. Journal of Catalysis 2007;250: 94–101.
[49] Porta F, Prati L. Selective oxidation of glycerol to sodium glycerate with gold-on-carbon catalyst: an insight into reaction selectivity. Journal of Catalysis 2004;224:397–403.
[50] Kwon Y, Schouten KJP, Koper MTM. Mechanism of the catalytic oxidation of glycerol on Polycrystalline gold and platinum electrodes. ChemCatChem 2011;3:1176–85.